Advances in Catheter-Based Ultrasound Imaging

Intracardiac Echocardiography and the ACUSON AcuNav™ Ultrasound Catheter

T.L. Proulx[1], Diana Tasker[1], Judy Bartlett-Roberto[2]

1 Siemens Medical Solutions, USA, Ultrasound Division, Mountain View, CA
2 JBR Consulting, LLC, Danville, CA

Abstract — **Conventional transthoracic and transesophageal ultrasound imaging often cannot satisfy imaging requirements for many advanced catheter-based interventional cardiac procedures due to restricted access to the anatomy. Intracardiac echocardiography (ICE) can provide almost unrestricted access and has been shown to be very effective in accurately guiding interventional cardiac procedures by providing high quality visualization of intracardiac anatomy and intracardiac devices. ICE is steadily replacing transesophageal ultrasound as the preferred imaging tool for device guidance during atrial fibrillation treatment, valve repair and closure of atrial septal defects. This article provides a history of the ACUSON AcuNav™ Ultrasound Catheter, a discussion of key technologies employed and a review of the expanding range of clinical applications where ICE technology is utilized. We also discuss recent innovations in catheter-based ultrasound, such as three-dimensional (3D) tools for navigation and volume rendering, new imaging modalities like acoustic radiation force imaging (ARFI) and emerging applications for catheter-based ultrasound in the field of minimally invasive surgery.**

Keywords- Intracardiac echocardiography, ICE, ultrasound, catheter, interventional cardiology, atrial fibrillation, RF ablation.

I. INTRODUCTION

Development of the ACUSON AcuNav™ Ultrasound Catheter began with a rigid 24 Fr. prototype to support proof of principle of intracardiac imaging efficacy. The first 7.0 MHz 128 element intracardiac probe (4 x 14mm array), shown in Fig. 1 was introduced to the right atrium via the jugular vein. The image quality of the cardiac anatomy and visualization of intracardiac devices located in the heart was so promising that an effort to assess the feasibility of a flexible 16 Fr. prototype was undertaken. The second prototype (7.0 MHz, 64 element, 4 x 7mm array) was mechanically more consistent with a catheter-based ultrasound probe and it too demonstrated high quality images. Given these successes, the AcuNav catheter development program was officially funded in late 1996 and after four years of development, the 10 Fr. 90 cm AcuNav™ ultrasound catheter received FDA clearance in late 1999 and was introduced to the market by Acuson (now Siemens Medical Solutions) in mid-2000. The production volume has grown exponentially from 50 catheters produced in the first quarter to more than 3500 catheters manufactured per quarter presently.

Since its introduction, a growing number of peer-reviewed journal articles have been published that point to the effectiveness and safety of the AcuNav catheter for procedures that include transcatheter closure of atrial level defects, visualization of ablation of anatomically-based supraventricular tachycardia ablation, and pulmonary vein isolation [1-10]. The numerous benefits cited include the ability to guide transseptal catheterization, assist in the placement of intracardiac devices such as mapping and ablation catheters and closure devices, monitor blood flow changes after therapeutic interventions, observe morphologic changes in ablation lesions to determine their effectiveness, and perhaps most importantly, early and instant detection of procedure-related complications, which allow for timely implementation of reparative measures.

Figure 1. Rigid 24 Fr. AcuNav prototype (top) compared to one of the current products, a 10 Fr. version.

While utilization of the AcuNav catheter in electrophysiology (EP) and interventional cardiology continues to grow, advancements in ultrasound transducer design and functionality, new imaging modalities and clinical applications are being intensively researched. This paper offers an introduction to the AcuNav ultrasound catheter, a review of the existing clinical applications for ICE and a discussion of some of the advanced technologies that are expected to change the field of catheter-based ultrasound thereby dramatically increasing its utility within the heart and throughout the body.

II. The AcuNav Ultrasound Catheter

A. Description

The AcuNav catheter contains a 64 element, 7.0 MHz phased array ultrasound transducer mounted on the tip of a single-use catheter available in 10 Fr. (90 cm insertable length) and 8 Fr. (110 cm) sizes. A photograph of the products in Fig. 2 shows the two catheters along with the disposable steering mechanism.

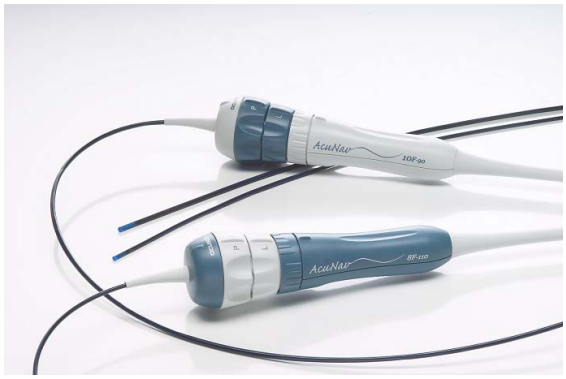

Figure 2. Photograph of AcuNav 8 Fr. and 10 Fr. ultrasound catheters (Siemens Medical Solutions, USA)

The entire device is connected to the ultrasound system via a SwiftLink™ catheter connector. The main components are diagrammed in Fig. 3.

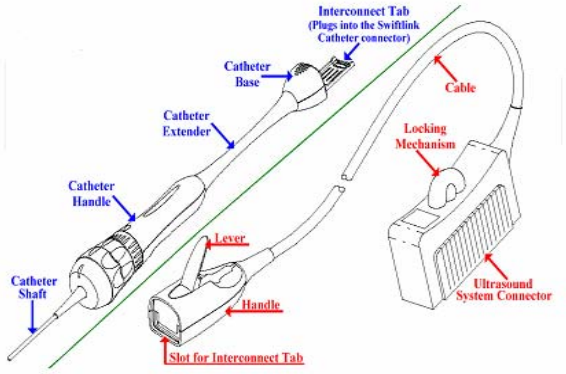

Figure 3. Diagram of the major device components

B. The Catheter and Transducer

The catheter component of the device consists of five basic sections: (1) the ultrasonic transducer, (2) a distal tip housing the transducer, (3) an anchor for terminating the control lines, (4) a braided deflectable section, and (5) a braided main body. The distal section is diagrammed in Fig. 4.

The 7.0 MHz array has 64 elements at 110 µm pitch (7.0 mm azimuth) and measures 2.0 mm (8 Fr. device) or 2.5mm (10 Fr. device) in the elevation direction. It is comprised of piezoelectric (PZT) ceramic with two acoustic matching layers mounted onto a very thin attenuating substrate (approx. 0.5 mm thick). The PZT is connected electrically by gold-plated flexible printed circuits, which are laminated to each side. The flex circuits, which contain the individual traces to the transducer elements, are folded underneath the transducer and backing substrate and extend out of the distal tip to run inside the length of the catheter. The traces are on a 100 µm pitch (50 µm trace, 50 µm space) in a signal-signal arrangement sandwiched by ground planes, resulting in a characteristic impedance of about 105Ω and capacitance of 90 pF/m.

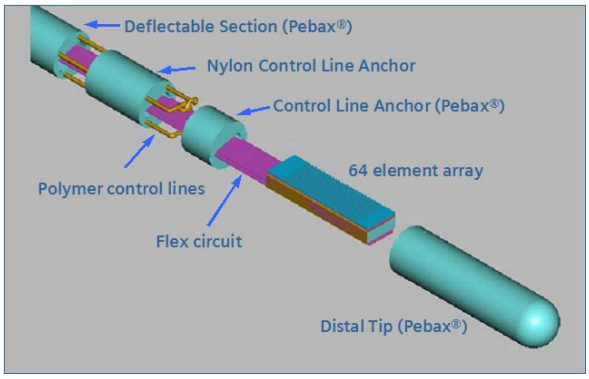

Figure 4. Diagram of the distal section of the catheter

The transducer assembly is mounted within the distal tip of the catheter, which is composed of Pebax® (Arkema Group, Paris, France) thermoplastic material. This tip acts as a flexible, durable, non-focusing acoustic window for the transducer. A typical time waveform and frequency spectrum for the 8 Fr. transducer element is shown in Fig. 5. The dual matching layer design results in 70-80% fractional –6dB bandwidth centered at 6.8 MHz.

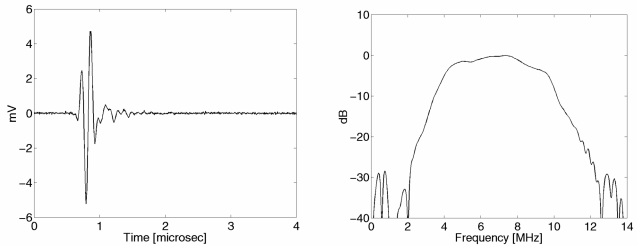

Figure 5. Typical time (a) and frequency response (b) of the 8 Fr. AcuNav catheter, based on roundtrip water tank measurements.

The deflectable section of the catheter is made from a low modulus Pebax to provide the flexibility needed to prevent damage to the surrounding tissue. This flexible section allows the catheter to deflect in two orthogonal planes: left-right (in a plane perpendicular to the image plane) and anterior-posterior (in a plane coincident with the image plane). It has five lumens: four circular lumens for the individual steering lines and a larger slot for the electrical conductors. The steering control lines, which are stranded polymeric material, pass through these lumens to a nylon anchor section. Each control line passes through a corresponding lumen in the anchor, where a knot is placed in the line to secure it in position, and then the line is passed back through an opposing lumen. A separate cap

of Pebax material is then fused over the anchor section to secure the lines in place. This anchor subassembly is then thermally fused to the deflectable catheter section.

The catheter main body is made of four lengths of increasingly higher modulus materials to provide appropriate torsional and bending characteristics and enough strength for insertion and placement of the catheter. The distal section is composed of lower modulus materials to match the flexibility of the deflectable catheter portion. The catheter main body subassembly is thermally fused to the distal tip portion of the catheter to form a completed catheter.

C. *Steering Mechanism*

Another major component of the AcuNav catheter is the disposable steering mechanism. The catheter is mounted and bonded into the distal end of the steering control mechanism, which is comprised of the steering control knobs, a tension knob, housing components, and the interconnect tab and flexible circuit. A schematic is given in Fig. 6.

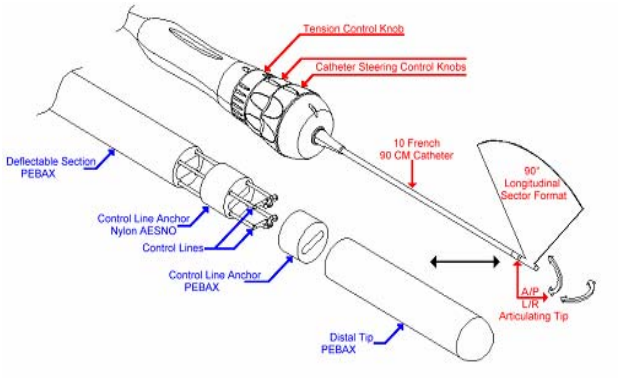

Figure 6. Diagram of the steering components of the catheter.

The steering control knobs deflect the catheter in two planes (left/right and anterior/posterior). For each plane of deflection, a pair of control lines from the catheter is routed inside of the mechanism around opposite sides of an inner hub with stainless steel pins attached. Each of the two hubs is connected to a steering-control knob. As the control knob is rotated within the hub, tension is applied to one control line while providing slack to the other, allowing the distal portion of the catheter to deflect in one direction. Rotating the knob in the opposite direction deflects the catheter in the opposite direction. Proximal to the steering control knobs is a third knob, which controls the tension applied to the steering knobs. By rotating this knob, a variable amount of friction can be applied to the steering control knobs to hold the distal catheter fixed in a curved position, with the degree of curvature selected by the physician.

D. *SwiftLink Catheter Connector*

The reusable SwiftLink catheter connector has three subcomponents: a shielded 2.5m cable, a connector for mating to the ultrasound system and a catheter connector for interconnection to the disposable catheter control housing. The shielded cable has 68 insulated coaxial conductors. The signal lines and the served coaxial shields are terminated at each end to printed wiring boards housed within the system connector and the catheter connector. An overall braided shield surrounds the individual coaxial conductors and is also connected to the printed wiring boards at each end.

E. *Volume Manufacturing and Regulatory Considerations*

In addition to the technical hurdles that were overcome to develop a phased array ultrasound transducer fitted within a 2.5 mm diameter lumen, relatively high volume production (10 to 15 thousand units per year) of a disposable device poses numerous manufacturing challenges. Significant efforts were required to develop the flexible circuits for the transducer array and for interconnecting the transducer array to the catheter proximal end connector, the acoustic backing material with adequate attenuation at 4.0 MHz when limited to 0.5 mm in thickness, the polymer control lines with sufficient tensile strength for articulation when limited to 0.23 mm in diameter, the disposable steering mechanism, and the catheter mechanical aspects to deploy the transducer safely in the right and left atria.

Since this device is considered Class II by the FDA, there are also numerous regulatory concerns that have been addressed. The AcuNav catheter conforms to more than sixty product safety standards in the areas of biocompatibility, clinical aspects, electrical safety, environmental aspects, EMC and radiation, labeling, mechanical safety, packaging, quality, risk management, and sterilization. Sterilization and packaging required for sterile medical devices are not typical ultrasound transducer areas of concern. While not difficult to implement, these areas are highly regulated and require significant validation. One of the key standards for catheter mechanical safety is EN10555: *Sterile, single-use intravascular catheters*, which applies to the integrity of catheter joints. Compliance with EN10555 can be a challenge not only for the catheter design, but also for the production joint forming processes. Catheter electrical safety also extends into new territory with considerations relating to the ability of the device to withstand defibrillation and retain dielectric breakdown performance with 0.125 mm polymer wall thicknesses.

III. Clinical Applications

A. *Electrophysiology*

The last several decades have brought about numerous changes in the treatment of complex arrythmias, none more important than improved visualization of therapeutic procedures through several methods. As the realization that different electrical signals of the heart (normal or aberrant) could be reliably associated with particular anatomical locations, the need for improved visualization of these targets rapidly became apparent. Electroanatomical mapping provides physicians with a pseudo 3D image of the chambers of the heart from which to guide the radiofrequency (RF) lesion placement. This method does not provide real time information, blood flow dynamics, tissue information, or information about the presence of complications. ICE, although two-dimensional in nature, addresses all of these limitations and is considered adjunctive to electroanatomical mapping.

Figure 7. Typical electrophysiology lab setting

Atrial fibrillation (AF), the most significant irregular heart rhythm due to the large proportion of affected people, is thought to have an anatomical association within the pulmonary veins or around the orifice of the pulmonary veins [11]. Treatment is through either pharmacology, ablation of the aberrant cells or a combination of both approaches. Pharmacologic treatment is expensive and produces undesirable side effects such that adherence to the drug regime is often difficult and sporadic. Left untreated, AF causes blood to clot in the left atrium, which can then travel to the brain, potentially causing stroke. The consequences are devastating for the patient and taxing on the health care system because of the costs involved.

Abolishing the aberrant electrical pathways through the placement of RF energy has gained widespread acceptance over the last several years as the curative treatment of choice, largely because of the availability of ICE to guide the procedure, thereby increasing efficacy and safety of a once "blind" procedure. Once associated with complications such as left atrial perforation and pulmonary vein stenosis, such complications are now rare as the physician is able to view the placement of the RF lesions in relation to critical cardiac anatomy. Fig. 8 compares still images of the same procedure taken with fluoroscopy and with ICE. Note the increased anatomical information available in the ultrasound image as compared to the fluoroscopy image.

As opposed to fluoroscopy and electroanatomical mapping visualization modalities, ICE affords real-time monitoring of the patient's hemodynamic status throughout the procedure and the ability to react quickly to complications that do occur. Additionally, the physician is now able to assess the quality of the contact between the tip of the RF ablation catheter and the endocardial surface, which is the most critical success factor in efficacious lesion formation. The lack of contact between these two surfaces leads to ineffective lesions without enough volume to sustain a continuous line or block against the aberrant signal.

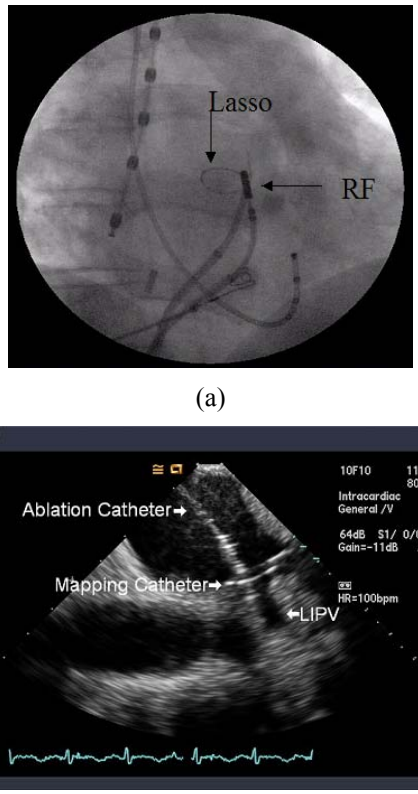

Figure 8. Fluoroscopy image (a) showing LASSO™ mapping cathether (Biosense Webster, Diamond Bar, CA) and RF ablation catheter compared to (b) an ICE image of the same view. The left inferior pulmonary vein (LIPV) is indicated on the ICE image.

B. Interventional Cardiology

Similar to the high incidence of AF in the EP lab, interventional cardiologists see a large number of patients with atrial level septal defects. Of the two main types, atrial septal defect (ASD) and patent foramen ovale (PFO), PFO is far more prevalent, affecting nearly 30% of the population with an incidence of 160,000 compared to 10,000 for the incidence of ASD. Both are characterized by a non-continuous atrial septum allowing abnormal flow of blood between the upper chambers of the heart.

Normally blood flows from the upper chambers to the lower chambers and the blood supply of the right heart, which is unoxygenated, is separated from the oxygenated left heart blood supply by the septum. In the case of PFO, the atrial septal tissue forms a flap that in the presence of increased intrathoracic pressure opens to allow unoxygenated blood to flow directly into the left atrium, bypassing the filtering function of the lungs. This may allow small particles of debris to flow into the left atrium and ultimately to the brain, potentially causing a stroke.

The abnormal blood flow pattern and septal appearance of an ASD is quite different. An ASD results from a true lack of septal tissue, and an opening is continually present in the septum regardless of intrathoracic pressures. Since the blood pressure in the left side of the heart is higher, blood flows

easily from the left side through the defect into the lower pressure right atrium, causing blood volume overload and extra work for the right heart. Over time, this continually present overload works the lungs and right ventricle of heart and a life-threatening condition called pulmonary hypertension may result. Fig. 9 shows ICE images of a PFO and ASD, demonstrating characteristic blood flow between the left and right atrium.

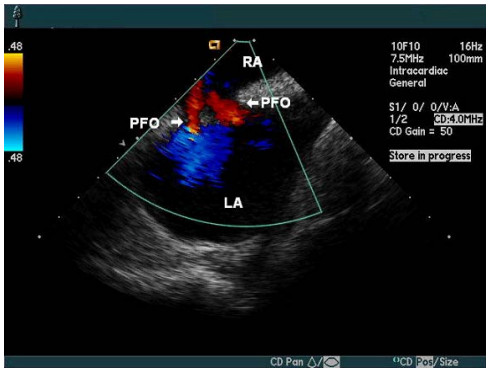

(a)

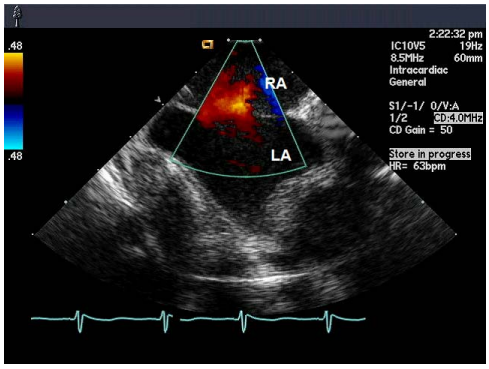

(b)

Figure 9. ICE color Doppler images showing examples of (a) PFO and (b) ASD.

Traditional treatment of PFO and ASD is open surgical repair in which a mesh screen is sewn directly onto the defective portion of the septum. Over time, fibrin adheres to the screen closing off the communication of the blood supply between the two upper chambers of the heart and thereby forcing flow into the normal cardiac pattern. This approach carries with it the complications, morbidity, expense, aesthetic disfiguration and extended recovery period of any open-chest surgical heart repair.

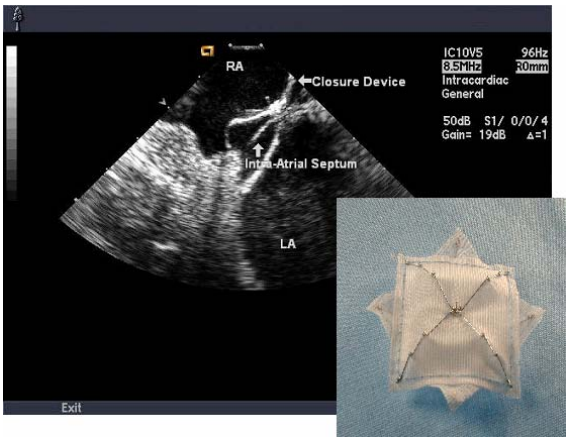

Figure 10. Photograph of the CardioSEAL® PFO closure device (NMT Medical, Boston, MA) and B-mode ICE image of the device after deployment in the intra-atrial septum

Since 1996, several companies have made significant headway in the creation of devices designed to close the septal defect in a non-invasive manner. Usually made of nitinol mesh and delivered percutaneously, a portion of the device sits on either side of the septal tissue present, and again, fibrin adheres to the mesh and prevents abnormal blood flow between the atria. A photograph of one of these PFO closure devices (NMT Medical, Boston, MA) and an ICE image after its deployment in a patient is shown in Fig. 10.

The success of percutaneous device placement is dependent upon adequate visualization of the septal tissue remaining, visualization of intracardiac anatomy (since other anatomical defects may also be present with ASD or PFO), accurate sizing of the defect so that an optimal size device is chosen, and finally characterization of blood flow patterns before and after device placement.

Before the availability of ICE, transesophageal echocardiography (TEE) was the visualization method of choice. The TEE probe is placed inside the esophagus and lowered to the level of the atria, necessitating the need for endotracheal intubation and general anesthesia with its accompanying risk and discomfort. Although omniplane in nature, the imaging planes are limited by the confines of the esophagus, a constraint ICE does not face since it is placed directly into the 3D space of the right or left atrium. Several studies have directly compared the quality and usefulness of the images obtained [7,12] and although little difference in image quality exists, those obtained by ICE provided a better assessment of the rim of tissue available for device placement for ASD closure.

C. Future ICE Applications

Future applications within the field of EP may include assisting in the placement of pacing leads into the coronary sinus and other areas of the cardiac venous structure for patients in congestive heart failure. Today, placement of leads is hampered by the lack of real time assessment of the myocardial response to the electrical stimulation provided by the pacing lead. Ideally, lead placement would be refined until optimal endocardial response was achieved.

Additional interventional applications under investigation include the placement of devices to occlude the left atrial appendage, guidance of percutaneous mitral valve repair [13] and aortic valve stent implants [14], all of which require the benefits of real time imaging, the high quality images and unlimited access to imaging planes afforded by placement of the echocardiography transducer directly into the cardiac chambers.

IV. Emerging Technology

A. New Clinical Applications and Imaging Modalities

As the clinical utility of ICE with the AcuNav catheter continues to be demonstrated in EP and interventional cardiology procedures, new applications for catheter-based ultrasound inside and outside the heart[1] are being investigated. Orsini et al. [15] have successfully used the AcuNav device for TEE as a way to minimize patient discomfort while Kew and Davies [16] report on the use of AcuNav catheter for visualization of the liver to guide hepato-portal vein punctures during transjugular intrahepatic portosystemic shunt (TIPS) procedures. Other researchers have investigated a side-viewing ultrasound cathether for endobronchial imaging [17] and the AcuNav catheter has shown promise for guiding renal stenting procedures as well as stent installation during abdominal aorta aneurism (AAA) repair procedures.

In addition to the color and spectral Doppler imaging available with the AcuNav catheter, advanced imaging modes such as Dopper Tissue Imaging (DTI) and velocity vector imaging (VVI) are being investigated for use in ICE applications. Research is also currently being applied to acoustic radiation force imaging (ARFI) with the AcuNav catheter [18] and some promising results have been achieved for monitoring lesion growth during RF ablation procedures.

B. Multi-Purpose Catheters

Stephens et al. [19] have built and tested a 9 Fr. combination intracardiac imaging and EP mapping catheter comprised of a 64 element phased array and multiple ring electrodes for measuring local electrical potentials. A similar device could in principle incorporate RF ablation electrodes as a means to reduce the number of catheters required for the procedure, while potentially improving visualization. A forward-viewing ring-annular array design [20] proposed for intravascular ultrasound (IVUS) might also be used to improve guidance of EP procedures, with a separate RF ablation catheter inserted via the working port and the imaging array positioned within several millimeters of the ablation site. However, combination therapy and imaging catheters will require the puncture of the septum to reach the wall of the left atrium, unless accessible by an existing ASD or PFO, and this may restrict the catheter size to less than 8 Fr. Navigation to the therapy point by C-plane or forward looking volumes may also prove exceptionally challenging.

C. Three-Dimensional Imaging

Consistent with conventional transthoracic ultrasound imaging, significant effort has been applied in recent years [20-25] to development of 3D catheter-based ultrasound for improved visualization of intracardiac structure and vessel pathology and morphology as well as guidance of therapeutic and interventional procedures in the areas of ICE and IVUS. Given the extent of the effort, we should expect a number of ultrasound catheters in the next several years that are capable of generating quality forward or side-viewing 3D volumes of much of the anatomy that is accessible by the vascular system, coupled in some cases with therapeutic devices. Several approaches to 3D volume formation include the use of side-firing and end-firing 2D matrix arrays, end-firing 2D ring arrays, swept apertures and mechanically rotated 1D arrays.

1) Mechanical Rotation

To investigate 3D ICE, Siemens has recently collaborated with Hansen Medical, Inc. (Mountain View, CA) and Tomtec Imaging Systems (Unterschleissheim, Germany) for a work-in-progress imaging system that acquires a 20^o - 40^o by 90^o 3D intracardiac volume by mechanically rotating the AcuNav catheter from outside the body while the array is positioned in the right atrium. A photograph of the device hardware attached to an AcuNav catheter is shown in Fig. 11.

Figure 11. A 10F AcuNav catheter shown with rotation hardware (Tomtec Imaging Systems, Unterschleissheim, Germany) attached to the catheter steering mechanism.

A series of 2D images is acquired either by gated ECG, with subsequent volume rendering at multiple points in the heart cycle, or by rapidly sweeping the array during diastole to create a volume once per heart cycle, thereby creating a pseudo-real time 3D image. Fig. 12 shows a left atrial (LA) volume rendered using this system with gated-ECG acquisition. The left pulmonary veins (PV) are clearly visible. When put into motion, the LA morphology throughout the heart cycle can easily be ascertained. As with the standard AcuNav catheter, the system is capable of color flow imaging as shown in Fig. 12 (b), offering additional clinical utility.

[1] U.S. law restricts use of the AcuNav catheter outside the heart as investigational use only

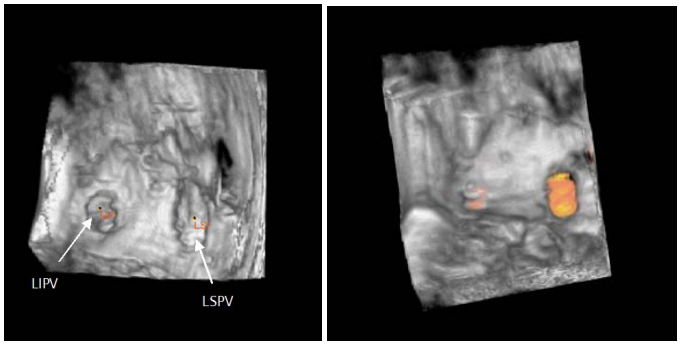

(a) (b)

Figure 12. AcuNav 3D ECG-gated volumes: (a) rendering of the left atrium wall showing the left inferior pulmonary vein (LIPV) and left superior pulmonary vein (LSPV), (b) left pulmonary veins with color flow

Fig. 13 shows the user interface for the rapid sweep through diastole and a 3D volume of the LA, showing the atrial appendage and a pulmonary vein. In this case, the 20^o x 90^o volume is updated once per heart cycle, potentially allowing improved device guidance during procedures.

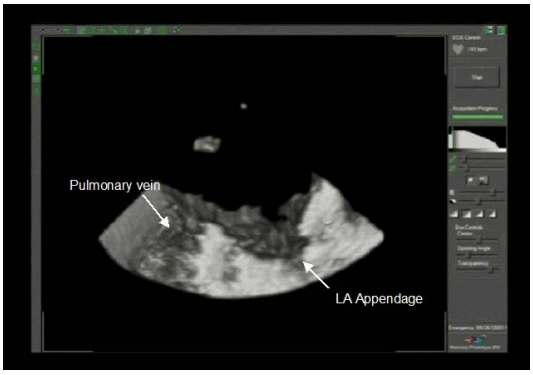

Figure 13. AcuNav 3D rapidly swept volume of the left atrium, showing the left atrial appendage and pulmonary vein

One drawback to this system is that rotation of the entire one meter catheter while inserted in the body in a torturous orientation can result in variable rotational frequency and therefore distortion of the image. This limitation may be addressed by moving the rotation to the distal tip. Miniature brushless DC motors have recently been developed (MicroMo Electronics, Clearwater, FL) with sufficient diameter (1.9 mm) and torque to fit inside an 8 Fr. catheter and rotate a 1D array at the catheter tip. Rotation could be via a flexible, low durometer section of catheter with a fixed array, as diagrammed in Fig. 14, or by using a floating array within a fluid filled catheter section.

2) Solid State 2D Arrays

Compared with the mechanically rotated 1D array, 2D arrays provide the ability to steer and focus the ultrasound beam in two dimensions over the entire volume, rather than only the azimuth plane, and produce much higher volume rates. Several groups have reported progress on development of 2D matrix and ring-annular arrays for intracardiac and intravascular imaging. The catheters vary in size from 5 Fr. with a 97 element end-firing 10 MHz matrix array for IVUS imaging [21] to 14 Fr. with a 112 element end-firing 5 MHz matrix array and a nearby working port for visualization of intracardiac therapy [22]. A 7 Fr. side-viewing catheter transducer with a 5 MHz, 112 element matrix array was fabricated and used to visualize the LA and pulmonary vein of a sheep while positioned in the coronary sinus [23].

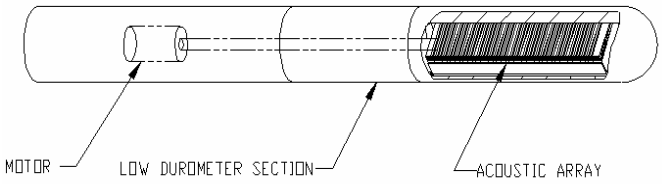

Figure 14. Schematic showing miniature motor and rotatable catheter tip for distal array wobbling.

Wang et al. have proposed and tested a ring-annular array consisting of 64 side-viewing and forward-viewing piezoelectric elements arranged around a 1.2 mm diameter ring [20, 24] for high frequency IVUS imaging with a central working port. Demirci et al. have also investigated a wideband CMUT version of this forward-viewing ring-annular array [25].

3) Swept Aperture Arrays

An alternate approach to a true solid state 2D array has recently been considered, where an elevation aperture consisting of strips of elements in the azimuth direction is swept over a convex radiused surface to produce a volume. The concept for a side-viewing swept aperture array is shown in Fig. 15 with 64 elements in azimuth divided into multiple segments in elevation.

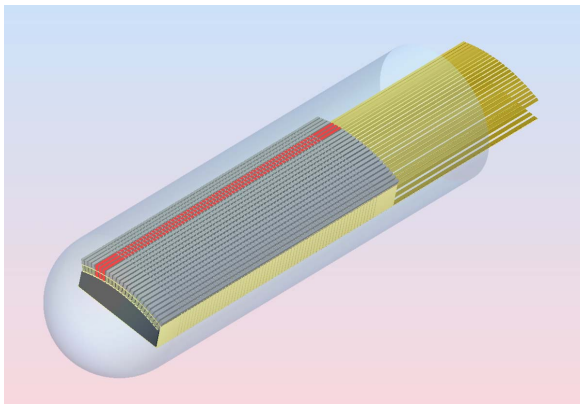

Figure 15. Side-viewing swept aperture catheter concept showing active elevation aperture in red.

The active elevation aperture (highlighted) intended for acquisition of a particular 2D image plane would be defined with a DC bias applied to either electrostrictive or CMUT elements. Successive 2D images would then be generated at different angles by sweeping the active elevation segments across the curved surface and a dynamic 3D volume constructed.

4) Spatial Resolution and Efficiency

The size restriction on the catheter body limits achievable performance for any intravascular or intracardiac ultrasound catheter, but the limits are more severe with 2D arrays. First, the lumen diameter defines the number of active transducer elements and thus the size or frequency of the array and the achievable spatial resolution. Additionally, the limited space effectively precludes use of impedance buffering electronics at the array. The small, high impedance 2D elements (2-5 pF) will be very inefficient at driving the 100-200 pF cable and will suffer significantly in terms of receive efficiency. Multi-layer ceramics may be used to increase element capacitance and improve the impedance matching, but extensive processing challenges make this technique unlikely for volume production.

Ultrasound cable technology has advanced considerably in recent years, and it is now possible to find 48AWG or smaller coaxes from several manufacturers (Precision Interconnect, Wilsonville, OR; Hitachi Cable, Tokyo, Japan), as well as miniature strip line cables [26] (MicroFlat®, W. L. Gore, Newark, DE) and a non-coaxial cable consisting of an arrangement of insulated wires (Precision Interconnect). As Table 1 shows, these non-coaxial technologies may allow a conductor count somewhere between 240 and 600 in a 10 Fr. catheter, depending on the type of RFI shielding, catheter cross section and desired flexibility.

TABLE I. ESTIMATED MAXIMUM SIGNAL COUNT FOR VARIOUS CABLE TYPES

Cable Type	*AWG / O.D. (mm)*	*Zc (Ω) / C (pF/m) / DCR (Ω/m)*	*Max signal count (estimated)*		
			8Fr	*10Fr*	*12Fr*
Coax	46 / 0.180	50 / 110 / 17	50	93	156
	48 / 0.160	50 / 110 / 30	63	117	198
	50 / 0.150	50 / 110 / 55	72	133	225
MicroFlat[A]	46	63 / 104 / 14.8	128	240	400
PI Comfort IS	48	>100 / 40 / 28	2.0-2.5[B]	2.0-2.5[B]	2.0-2.5[B]
	50	>100 / 40 / 46	2.5-3.0[B]	2.5-3.0[B]	2.5-3.0[B]
	52	>100 / 40 / 71	>300	>600	>900

[A] signal-signal configuration at 100 µm pitch with ground plane; estimate based on 50 signals / mm^2

[B] estimated proportional increase compared to 50Ω coax with same AWG conductor

Considering these limitations, we can compare estimated spatial resolution and receive efficiency of several theoretical 2D arrays in comparison to the benchmark AcuNav catheter transducer. Table 2 provides a description of the arrays along with simulated receive efficiency when loaded by a 2.3m cable of specified variety and a 50Ω receiver. The small, high impedance 2D elements are estimated at 20 – 25 dB worse on receive than the current AcuNav catheter, while the swept aperture shows much better performance due to the parallel combination of multiple elevation segments and use of a low capacitance flex circuit.

Spatial resolution in the C-plane was simulated using Field II [27] for each case. Figs. 16 and 17 show on-axis roundtrip point spread functions (PSF) and beamplots along the azimuth and elevation planes for selected frequencies and focal depths. Beamwidths are summarized in Table 3.

TABLE II. ARRAY DESCRIPTION AND ELEMENT RECEIVE EFFICIENCY

Type	Description	Element dims (mm)	Cath-eter	Cable type	Signal count	Receive sensitivity
AcuNav™	7mm x 2.5mm 1D array	0.085 x 2.6	10Fr	Flex circuit	64	0dB
Swept	64 elements, 20 elev segments, 1.0mm active aperture	0.085 x 1.0	10Fr	Flex circuit	84	-4.6dB
Ring-annular	10MHz end-fire, 2.6mm OD, 2.0mm ID, 128 elem @ 55µm pitch	0.055 x 0.300	10Fr	48AWG IS	128	-21.6dB
Ring-annular	same	0.055 x 0.300	10Fr	46AWG Strip	128	-22.6dB
Matrix 2D	7MHz 2.7 x 2.4mm array (21 @ 130µm, 12 @ 200µm pitch)	0.085 x 0.150	10Fr	50AWG IS	252	-24.6dB

In the near field (1 cm), both the ring-annular and matrix arrays improve the elevation resolution of the AcuNav catheter by a factor of about two, with a corresponding factor of two reduction in azimuth resolution. The ring-annular array has a high clutter level that may be improved using a synthetic aperture technique [24].

At a depth of 4 cm, the matrix array forfeits its advantage in elevation, matching the AcuNav catheter performance, while maintaining its worse azimuth resolution. In contrast, the swept aperture array could in principle achieve the same azimuthal resolution as the existing AcuNav catheter, with somewhat diminished elevation resolution at the cost of only 15-20 additional conductors.

The 3D image quality of the mechanically rotated 1D AcuNav catheter, despite its relatively poor elevation beam characteristics, has shown considerable promise for device visualization and guidance and assessment of morphology, as evidenced by Figs. 12 and 13. Allowing for reduced penetration when compared to the AcuNav catheter, the results presented in Tables 2 and 3 indicate that a 2D array alternative may provide sufficient performance to allow for a true 4D solution for catheter-based ultrasound.

TABLE III. PROJECTED BEAMWIDTH IN ELEVATION AND AZIMUTH (mm)

Type	Focus (mm)	Freq (MHz)	Elevation		Azimuth	
			-10dB	-30dB	-10dB	-30dB
AcuNav	40	7	4.0	11.3	1.4	2.8
Swept	40	7	8.0	13.9	1.4	2.8
Matrix 2D	40	7	4.1	7.0	3.6	10.5
AcuNav	10	10	1.4	4.3	0.3	0.8
Ring-annular	10	10	0.6	3.3	0.6	3.3
Matrix 2D	10	10	0.75	2.0	0.65	1.8

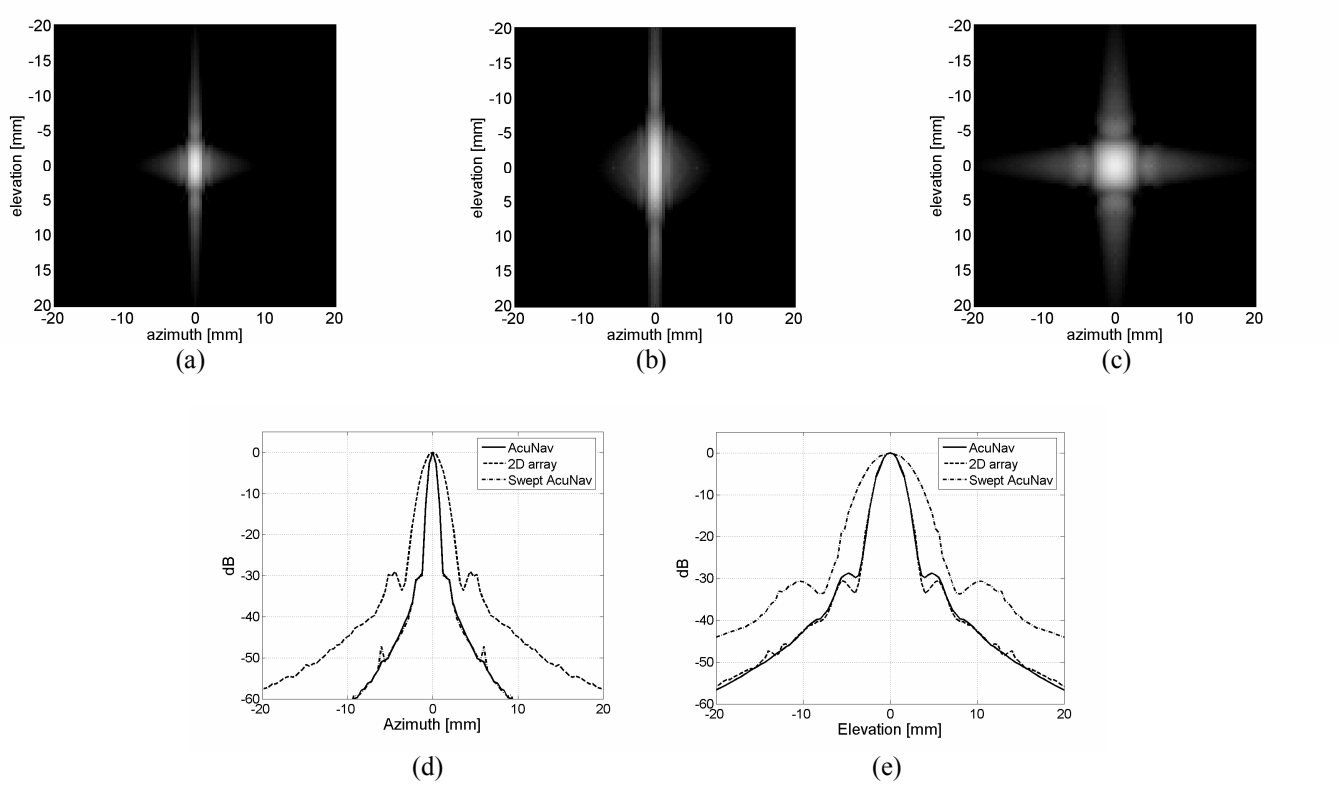

Figure 16. Field II simulation of C-plane PSF at 7MHz, 4cm focus for (a) existing AcuNav 10 Fr. catheter, (b) swept aperture, (c) 2D matrix array; projected intensities on azimuth (d) and elevation (e) planes

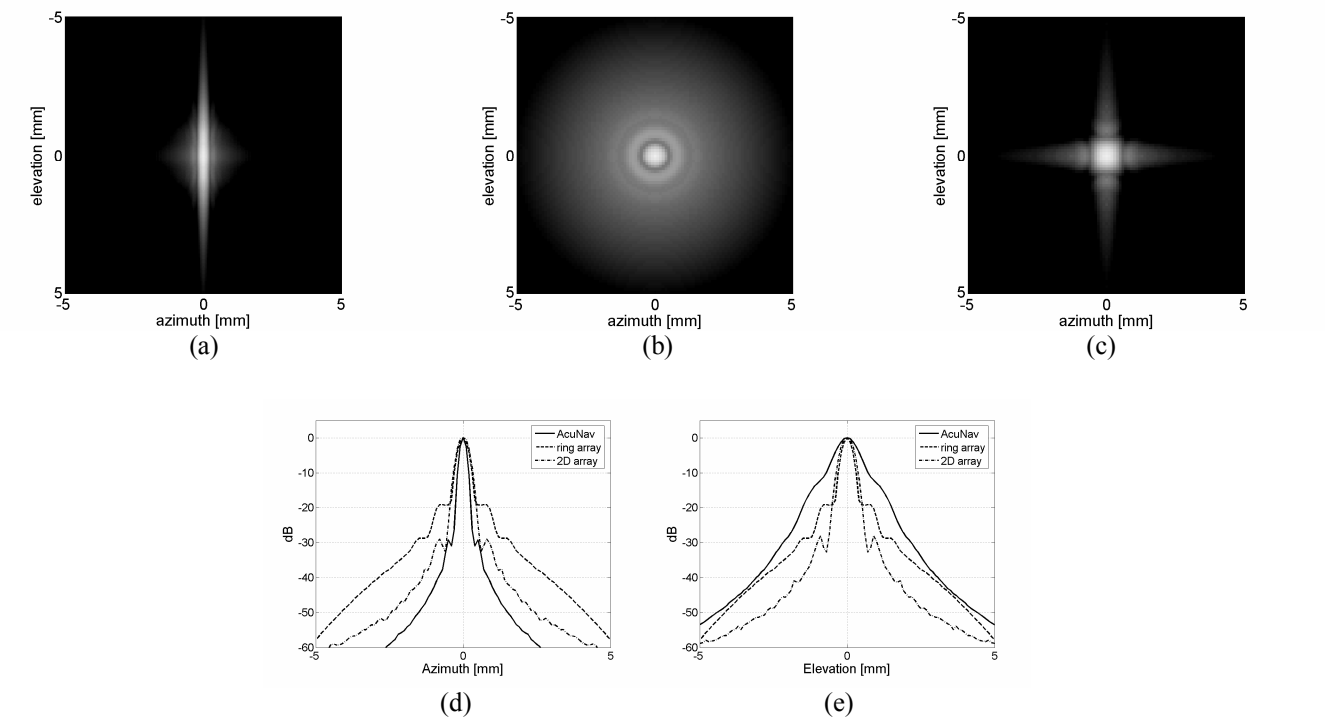

Figure 17. Field II simulation of C-plane PSF at 10 MHz, 1cm focus for (a) existing AcuNav 10 Fr. catheter, (b) ring-annular array, (c) 2D matrix array; projected intensities on azimuth (d) and elevation (e) planes.

V. CONCLUSION

There is little doubt that the high resolution, phased array imaging provided by the AcuNav ultrasound catheter has dramatically changed the standard of care for complex electrophysiology and interventional cardiology procedures. Additional development is needed however if physicians and patients are to truly benefit from this real time imaging mode. Imaging three-dimensional anatomy with a two dimensional imaging tool requires advanced training and a case load sufficient to master the intricacies of the learning curve. Visualization of the therapeutic device and its relation to target cardiac anatomy is of paramount importance. Real time 3D intracardiac ultrasound offers the potential to simplify image acquisition and interpretation, improving the ease of device guidance, reducing both procedure and fluoroscopy time and improving patient outcomes. The combined procedural volume for established procedures such as atrial fibrillation ablation and PFO/ASD closure are sufficient to warrant the investment by industry to refine this technology.

REFERENCES

[1] D. L. Packer, et al., "Intracardiac phased-array imaging: methods and initial clinical experience with high resolution, under blood visualization," *J. Am. Coll. Cardiology*, Vol. 39, pp 509-516 (2002).

[2] M. G. Earing, et al., "Intracardiac echocardiography guidance during transcatheter device closure of atrial septal defect and patent foramen ovale," *Mayo Clin. Proc*., Vol. 79, pp 24-34 (2004).

[3] G. P. Ussia, A. Privitera, M. Campisi, M. Carminati, F. De Luca, "Intracardiac echocardiography using the AcuNav™ ultrasound catheter during percutaneous closure of multiple atrial septal defects," *Ital. Heart Journal*, Vol. 5, pp 392-395 (2004).

[4] Z. Liu, et al., "Catheter-based intracardiac echocardiography in the interventional cardiac laboratory," *Catheter Cardiovasc. Interv*., Vol 63, pp 63-71 (2004).

[5] I. Sheikh, et al., "Novel uses of intracardiac echocardiography with a phased-array imaging catheter," *J. Am. Soc. Echocardiography*, Vol. 16, pp 1073-1077 (2003).

[6] D. S. Beinborn and K. Monahan, "Usage of Acuson AcuNav imaging during complex ablations," *EP Lab Digest*, Vol. 3, pp 30-33 (2003).

[7] P. Koenig, Q. L. Cao, M. Heitschmidt, D. J. Waight, Z. M. Hijazi, "Role of intracardiac echocardiography guidance in transcatheter closure of atrial septal defects and patent foramen ovale using the Amplatzer device," *J. Interv. Cardiology*, Vol. 16, pp 51-62 (2003).

[8] J. F. Ren, F. E. Marchlinski, D. J. Callans, E. S. Zado, "Intracardiac Doppler echocardiographic quantification of pulmonary vein flow velocity: an effective technique for monitoring pulmonary vein ostia narrowing during focal atrial fibrillation ablation," *J. Cardiovasc. Electrophysiology*, Vol 13, pp 1076-1081 (2002).

[9] J. F. Ren, F. E. Marchlinski, D. J. Callans, H. C. Herrmann, "Clinical use of AcuNav diagnostic ultrasound catheter imaging during left heart radiofrequency ablation and transcatheter closure procedures," *J. Am. Soc. Echocardiography*, Vol 15, pp 1301-1308 (2002).

[10] I. T. Dairywala, et al., "Catheter-based interventions guided solely by a new phased-array intracardiac imaging catheter: in vivo experimental studies," *J. Am. Soc. Echocardiography*, Vol 15, pp 150-158 (2002).

[11] E. Saad, N. Marrouche, A. Natale, "Ablation of atrial fibrillation," *Current Cardiology Reports*, Vol. 4, pp. 370-387 (2002)

[12] Z. M. Hyjazi, Z. Wang, Q. Cao, P. Koenig, D. Waight, R. Lang, "Transcatheter closure of atrial septal defects and patent foramen ovale under intracardiac echocardiographic guidance: feasibility and comparison with transesophageal echocadiography," *Catheterization and Cardiovasclar Interventions*, Vol. 2, pp 194-199 (2001).

[13] M. I. Salem, et al., "Intracardiac echocardiography using the AcuNav ultrasound catheter during percutaneous balloon mitral valvuloplasty," *J. Am. Soc. Echocardiography*, Vol. 15, pp 1533-1537 (2002).

[14] C. H. Huber, M. Nasratulla, M. Augstburger, L. K. von Segesser, "Ultrasound navigation through the heart for off-pump aortic valved stent implantation: new tools for new goals," *J. Endovasc. Ther*., Vol. 11, pp 503-510 (2004).

[15] A. N. Orsini, T. J. Kolias, K. R. Strelich, W. F. Armstrong, "Feasibility of transesophageal echocardiography with a ten-French monoplane probe," *J. Am. Soc. Echocardiography*, Vol. 16, pp 682-687 (2003).

[16] J. Kew, R. P. Davies, "Intravascular ultrasound guidance for transjugular intrahepatic portosystemic shunt procedure in a swine model," *Cardiovasc. Intervent. Radiology*, Vol. 27, pp 38-41 (2004).

[17] O. Clade, F. Tranquart, M. Olar, E. Hazouard, D. Diner, "10MHz ultrasound linear array catheter for endobronchial imaging," *IEEE Ultrasonics Symposium Proceedings*, pp 1942-1945 (2004).

[18] S. J. Hu, G. E. Trahey, Duke University, unpublished work.

[19] D. N. Stephens et al., "Clinical application and technical challenges for intracardiac ultrasound imaging", *IEEE Ultrasonics Symposium Proceedings*, pp 772-777 (2004).

[20] Y. Wang, D. N. Stephens and M. O'Donnell, "Initial results from a forward-viewing ring-annular ultrasound array for intravascular imaging," *IEEE Ultrasonics Symposium Proceedings*, pp 212-215 (2003).

[21] E. D. Light, S. W. Smith and J. F. Angle, "Advances in two dimensional arrays for real time 3D intravascular ultrasound," *IEEE Ultrasonics Symposium Proceedings*, pp 790-793 (2004).

[22] W. Lee, S. F. Idriss, P. D. Wolf and S. W. Smith, "Dual lumen transducer proges for real-time 3-D interventional cardiac ultrasound," *Ultrasound in Medicine and Biology*, vol. 29, pp 1297-1304 (2003).

[23] W. Lee, S. F. Idriss, P. D. Wolf and S. W. Smith, "A miniaturized catheter 2-D array for real-time 3-D intracardiac echocardiography," *IEEE Transactions on Ultrasonics, Ferroelectrics and Frequency Control*, Vol. 51, pp 1334-1346 (2004).

[24] Y. Wang, D. N. Stephens and M. O'Donnell, "Optimizing the beam pattern of a forward-viewing ring-annular ultrasound array for intravascular imaging," *IEEE Transactions on Ultrasonics, Ferroelectrics, and Frequency Control*, Vol. 49, No. 12, pp 1652-1664 (2002).

[25] U. Demirci, A. S. Ergun, O. Oralkan, M. Karaman, B. T. Khuri-Yakub, "Forward-viewing CMUT arrays for medical imaging," *IEEE Transactions on Ultrasonics, Ferroelectrics, and Frequency Control*, Vol. 51, No. 7, pp 887-895 (2004).

[26] C. Oakley, J. Mueller, D. Dietz, J. Kuhnke, " A minimally invasive ultrasound probe using non-coax cabling," *IEEE Ultrasonics Symposium Proceedings*, pp 1011-1016 (2001).

[27] J. A. Jensen, N. B. Svendsen, "Calculation of pressure fields from arbitrarily shaped, apodized, and excited ultrasound transducers," *IEEE Transactions on Ultrasonics, Ferroelectrics, and Frequency Control*, Vol. 39, pp 262-267 (1992).